IJISET - International Journal of Innovative Science, Engineering & Technology, Vol. 1 Issue 10, December 2014.
www.ijiset.com
ISSN 2348 – 7968

Structural and Optical Properties of Synthesized Manganese doped ZnS Quantum Dots

Iftikhar M.Ali, Raad M.Al-Haddad, Khalid T. Al-Rasoul

University of Baghdad, College of Science, Department of Physics, Iraq, Baghdad

Abstract

$ZnS:Mn^{2+}$ nanoparticles were prepared by a simple microwave irradiation method under mild condition. The starting materials for the synthesis of $ZnS:Mn^{2+}$ quantum dots were zinc acetate as zinc source, thioacetamide as a sulfur source, manganese chloride as manganese source (R & M Chemical) and ethylene glycol as a solvent. All chemicals were analytical grade products and used without further purification. The quantum dots of $ZnS:Mn^{2+}$ with cubic structure were characterized by X-ray powder diffraction (XRD), the morphology of the film is seen by scanning electron microscopy (SEM) also by field effect scanning electron microscopy (FESEM). The composition of the samples is analysed by EDS. UV-Visible absorption spectroscopy analysis shows that the absorption peak of the as-prepared ZnS sample (310 nm) displays a blue-shift comparing to the bulk ZnS (345 nm).

1. Introduction

In terms of continuous miniaturization of electronic devices nanotechnology is a ray of hope for semiconductor industries due to peculiar properties of nano-materials that changes significantly the efficiency of the devices. Research in nanoscale materials get started because of the unique properties that are obtain at this scale, by changing the shape or size of these materials[1]. At nanoscale, the behavior of materials drastically get changed and hence their properties. Particularly in semiconductors, it results due to the motion of electron to a length scale that is equal or smaller to the length scale of the electron Bohr radius that is generally a few nanometers[2]. Wide-bandgap II–VI compounds have been applied to optoelectronic devices, especially light emitting devices in the short-wavelength region of visible light, because of their direct gap and suitable bandgap energies. Here our focus is on ZnS semiconductor which is studied in the present study. Zinc sulfide (ZnS) is one of the most typical and important crystalline materials for both application and research [3-5]. The most notable feature of nanosized ZnS particles is that its physical and chemical properties dramatically differ from that observed from bulk solid semiconductor, i.e. nanoparticles exhibit wider energy gap and quantum size confinement. ZnS occur in both Zinc Blend (ZB) and Wurtzite (WZ) crystal structure.

In undoped II-VI semiconductors (e.g., CdS, CdSe, and ZnS), the band gap can be tuned by controlling the particle sizes [6-8]. Research studies are carried out on doped II-VI semiconductor nanomaterials to enhance their light emission properties and thereby making them good candidate for optoelectronic applications [9-11]. The doping of ZnS with transition metals such as Mn, Cu, Ni, Fe and Ag is interesting to researchers because of the effect of dopant on the photoluminescence and photoreactivity properties of the semiconductor. Transition metal ions doped ZnS nanoparticles are the most popular materials for research in semiconductor nanocrystals. Doped nanocrystals of semiconductor can yield high luminescence [12]. These results suggested that doped semiconductor nanocrystals form

ISSN 2348 – 7968

a new class of luminescent materials, with a wide range of applications in displays, sensors and lasers [13].

2 Experimental

2.1 Instrumentation

A microwave oven with 1100 W power (LG) was used. Powder X-ray diffraction (XRD) pattern of prepared ZnS was recorded by diffractometer (SHIMADZU-XRD 6000) using a Cu Kα radiation (λ=1.5406Å). Morphology was examined by scanning electron microscope SEM) and Field Emission scanning electron microscope(FESEM). A Shimadzu UV-Vis spectrometer was used to record the UV-Visible absorption spectra (UV-1650PC SHIMADZU, Columbia, MD, USA).

2.2 Preparation of Mn doped ZnS Quantum Dots

The starting materials for the synthesis of Mn doped ZnS QDs were zinc acetate (R & M Chemical) as zinc source, thioacetamide as a sulfur source, manganese chloride as a manganese source and ethylene glycol as a solvent. In a typical synthesis, 5 mM of zinc source and 0.05mM of manganese source were added with appropriate concentrations of Manganese (1, 2, 3 and 4) wt.% in a glass beaker of 80 mL containing 20 mL of ethylene glycol and 60ml distilled water as solvent . The solution was stirred for 1hour 70^{o}C, and then 6 mM of sulfur source dissolved in 20ml was added by drop wise and stirred for 30 min. The beaker was placed in a high power microwave oven (1100 W) operated using a pulse regime with 20% power for 25 min irradiation time. The formed precipitates were centrifuged (4000 rpm, 10 min) and the residue was washed several times with distilled water and absolute ethanol. The products were dried in air at 60°C for 24 h under control environment and can be stored for extended period of time.

3 Result and discussion

3.1 Structural Analysis:

3.1.1 XRD Analysis

The XRD patterns of undoped and doped ZnS QDs are displayed in figure1. It can be identified as the cubic zinc blende structure with a comparison to the standard card (JCPDS, no. 05-0566). All the samples show the characteristic reflections from (111), (220), and (311) planes. No peaks corresponding to manganese compounds were observed, demonstrating that Mn ions are dispersed in ZnS matrix. Also No peaks corresponding to other impurities were identified in the pattern, indicating the high purity of the final product. The large width of the diffraction peaks is an indication of the nanosize of the particles. The crystallite size is calculated to be smaller than Bohr radius a_B , where Bohr radius for ZnS is 2.5nm, that means, we have quantum dot nanoparticles. So we have strong confinement in the wave function of the electron.

The three peaks of the XRD patterns of manganese-doped ZnS clearly show no shifting of the center of the diffraction peaks as seen in figure 1. The XRD corresponds to the light reflected from the planes where the periodic arrangement of the atoms is perfect and continuous [14]. The ionic radius of Mn^{2+} is 0.1 A˚ whereas that of Zn^{2+} is 0.74 A˚. As doping of Mn^{2+} does not appreciably disturb the plane, no change in XRD pattern is obtained.

ISSN 2348 – 7968

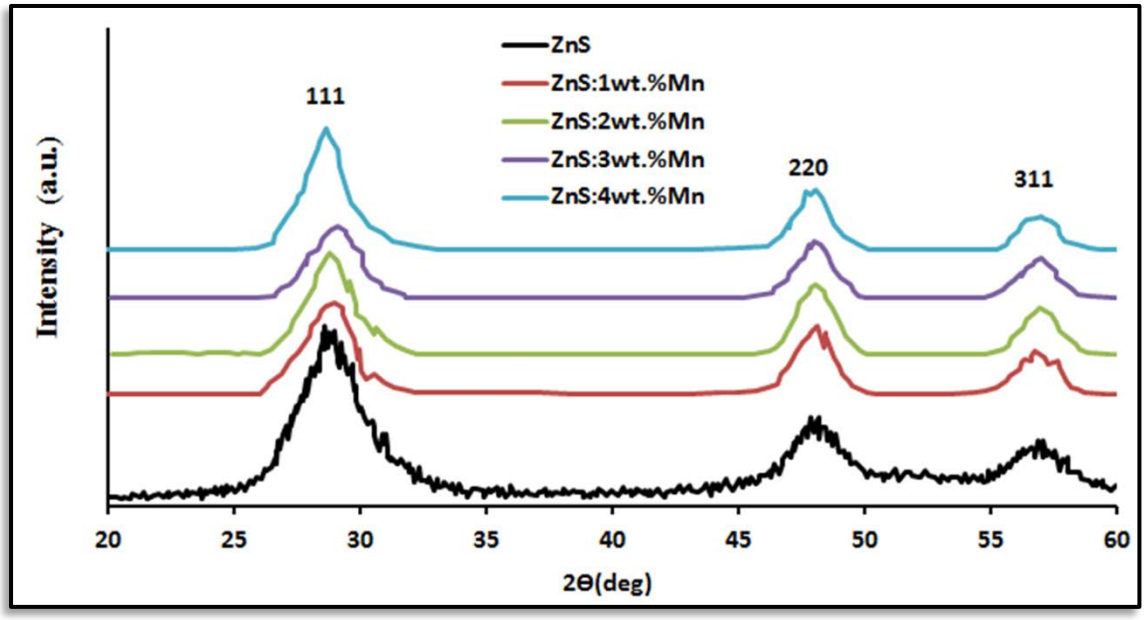

Fig.1 XRD patterns for undoped and manganese doped ZnS.

The FWHM of the XRD peaks may also contain contributions from lattice strain[11]. In nanocrystalline materials, there is microstrain broadening which is very common. Lattice strain arises from displacements of the unit cells about their normal positions which is often produced by dislocations, domain boundaries, surfaces etc[11]. Therefore, the average strain of the ZnS nanoparticles is calculated using Stokes-Wilson equation[12]:

$$\varepsilon_{str} = \beta\cot\theta / 4 \ldots\ldots\ldots\ldots (1)$$

Where β is the full width at half maximum (FWHM) of the diffraction peak (in radian), and θ is the diffraction angle. The d-spacing is calculated using the relation[14]:

$$d_{hkl} = n\lambda /2\mathrm{Sin}\theta \ldots\ldots\ldots\ldots (2)$$

where λ is the X-ray wavelength (here λ = 1.54060 Å).
The average crystallite size of the powder calculated by Debye-Scherrer's formula is estimated to be 2.19 nm through the Scherrer equation[10] after treating the broadening due to instrumentation and strain:

$$D=K\lambda/(\beta\cos\theta) \ldots\ldots\ldots\ldots\ldots (3)$$

Where K is the geometric factor (0.9). Also the dislocation density (δ) which represents the amount of defects in the sample is calculated using the relation[13]:

$$\delta = 1/D^2 \ldots\ldots\ldots\ldots\ldots\ldots (4)$$

where D is the average crystallite size. The lattice constant is estimated from the intercept of the Nelson-Riley plot (Fig. 2) which is a graph of the calculated values of lattice constant for different planes versus the error function given by[15]:

$$f(\theta) = \frac{1}{2}\left(\frac{\cos^2\theta}{\sin\theta} + \frac{\cos^2\theta}{\theta}\right) \ldots\ldots (5)$$

ISSN 2348 – 7968

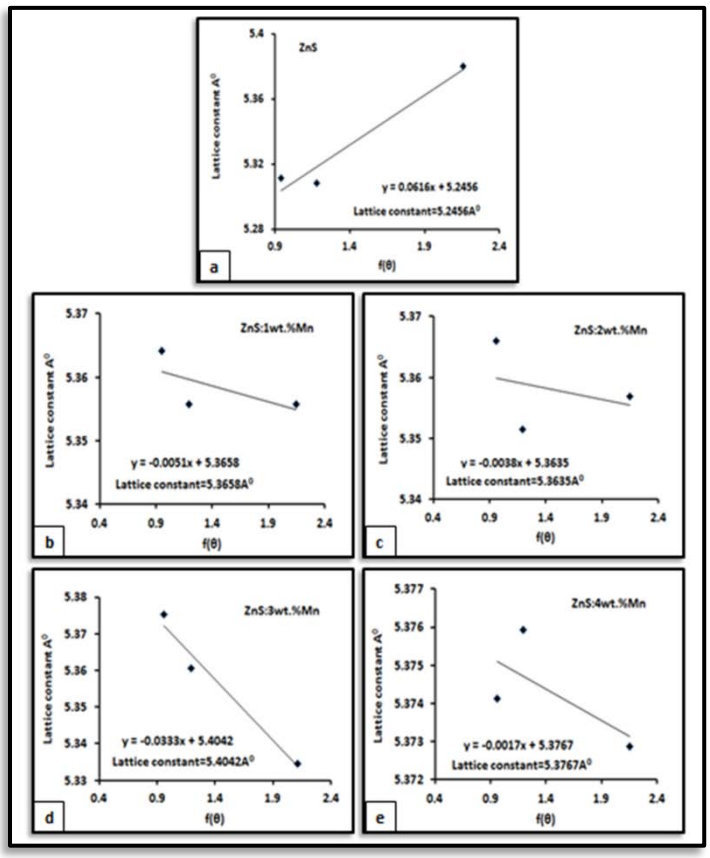

Fig. 2 Nelson-Riley plot of nanocrystalline Mn doped ZnS QDs; (a, b, c, d &e corresponding to (0, 1, 2, 3 & 4) wt.%Mn respectively).

The strain of ZnS nanoparticles is calculated from eq.(1) as shown in figure 3.

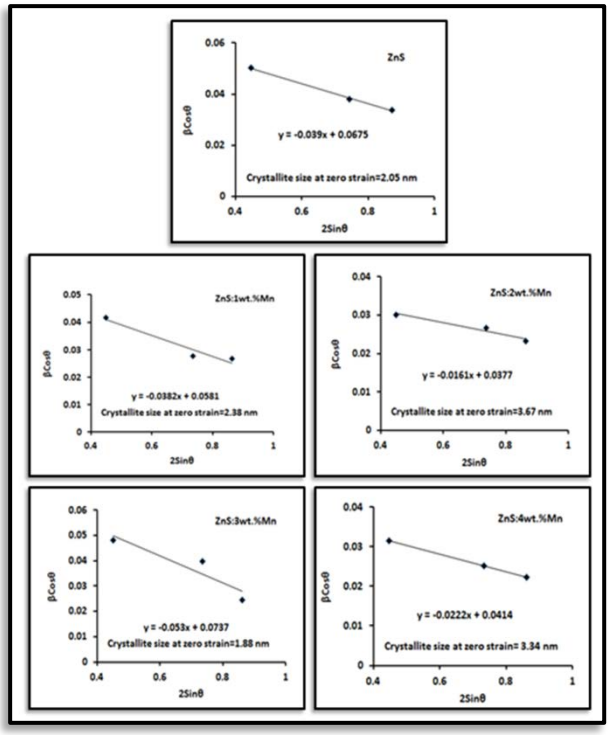

Fig. 3 Stokes-Wilson plot of nanocrystalline undoped and doped ZnS QDs.

ISSN 2348 – 7968

The calculated structural parameters are given in table-1.

TABLE 1 Structural Parameters of undoped and doped ZnS QDs

Sample	2θ (Deg)	Plane (hkl)	Interplaner Spacing d(A^0)	Lattice constant a(A^0)	FWHM (rad)	Average Crystalline Size D(nm)	Dislocation Density δ(lines/m^2) x10^{16}	Average Strain ε_{str}x10^{-3}
ZnS	28.7158 48.4664 57.5002	(111) (220) (311)	3.10632 1.87671 1.60149	5.2456	0.0514 0.0409 0.0375	2.05	23.7	14.5
ZnS:1wt.% Mn	28.8507 48.0083 56.8849	(111) (220) (311)	3.09210 1.89355 1.61734	5.3658	0.0427 0.0297 0.0296	2.38	17.5	38.2
ZnS:2wt.% Mn	28.8440 48.0492 56.8629	(111) (220) (311)	3.09281 1.89203 1.61791	5.3635	0.0309 0.0287 0.0257	3.67	7.3	16.1
ZnS:3wt.% Mn	28.9673 47.9625 56.7555	(111) (220) (311)	3.07992 1.89525 1.62072	5.4042	0.0497 0.0427 0.0270	1.88	28.3	53.0
ZnS:4wt.% Mn	28.7564 47.8168 56.7692	(111) (220) (311)	3.10203 1.90068 1.62036	5.3767	0.0322 0.0270 0.0246	3.34	8.9	22.2

We can conclude from the values tabulated in table-1 that the doping make distortion in the host lattice because the values of lattice constant vary significantly. Also we can see that the strain; as well as the dislocation density **δ;** increases with decreasing the crystallite size.

3.1.2 Field Emission Scanning Electron Microscope (FESEM) Analysis

Figure 4 illustrates pure ZnS nano powder at high and low magnifications. It is obvious that the prepared nanoparticles were found to be in cluster form. Also the surface morphology of undoped and doped ZnS nanoparticles have spherical shape (also see figure 5). In some places, various sizes of the particles (small and large size) are observed, i.e. nano-sized particles seem to be randomly distributed in the films and this observation also is seen by Tsunekawa et. al.[15].

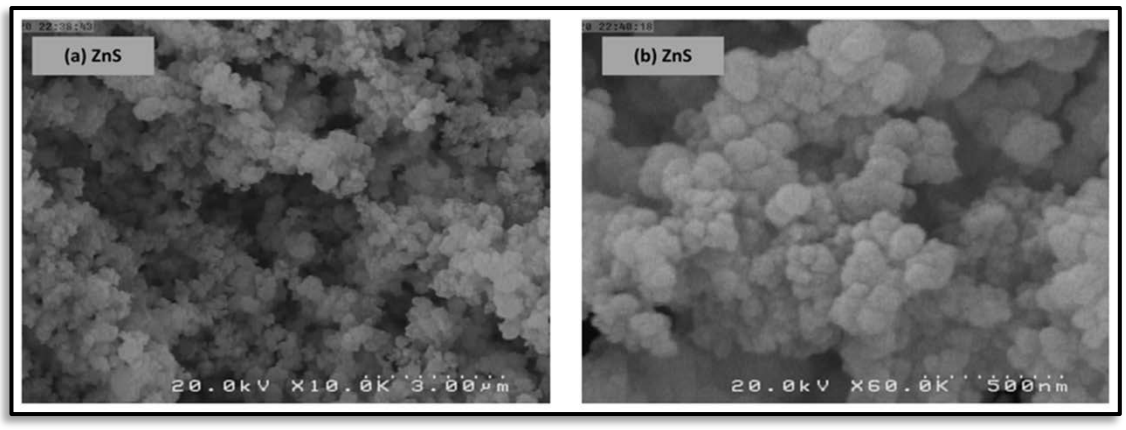

Fig. 4 FESEM images of ZnS QDs (a) low magnification, (b) high magnification.

ISSN 2348 – 7968

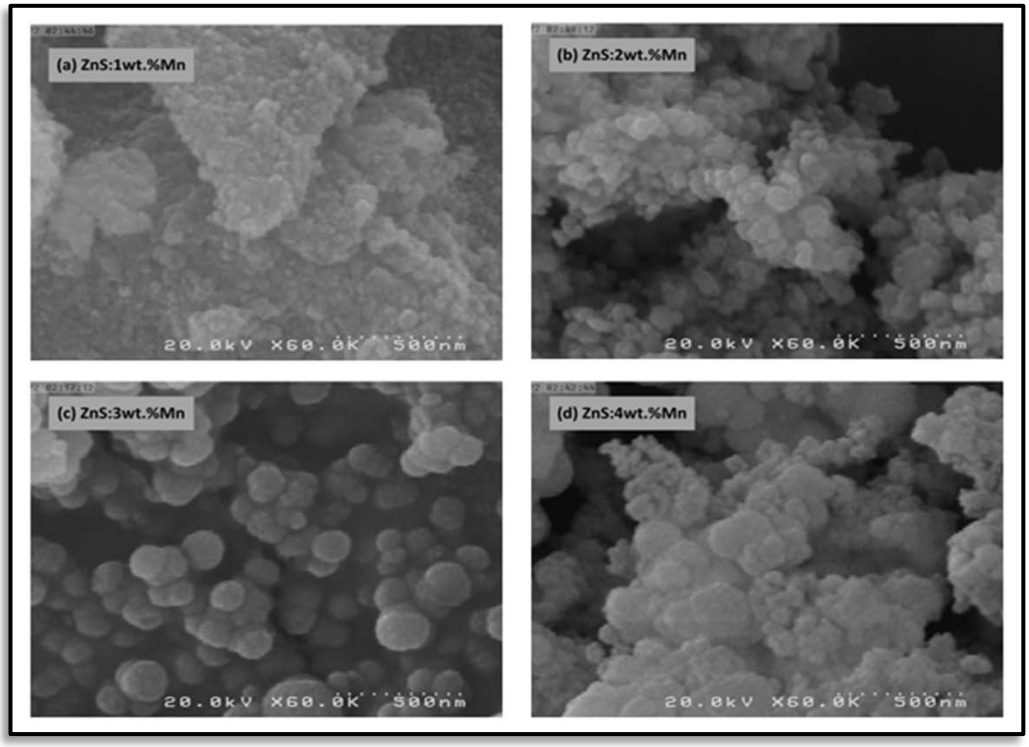

Fig. 5 FESEM images of Mn doped ZnS QDs; (a,b,c &d are corresponding to doping concentrations 1%, 2%, 3% and 4%) respectively.

High Resolution-FESEM Figure 6 is taken for zinc sulfide doped with manganese that proved we prepare nanoparticles at approximately less than 5nm (see figure 6b).

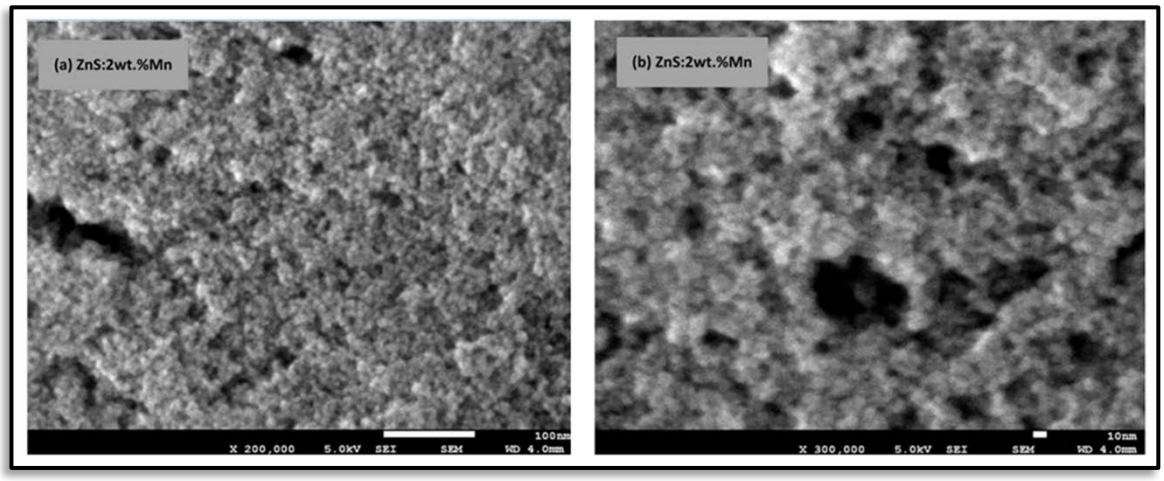

Fig. 6 HR-FESEM images of Mn doped ZnS QDs (a) low magnification, (b) high magnification.

3.1.3 Energy Dispersive Spectroscopy (EDS) Analysis

The composition of the samples is analyzed by EDS. Figure 7 illustrates EDS spectrum and shows the atomic percentage of Zn and S (other elements are not labeled). The result shows

ISSN 2348 – 7968

that the atomic percentages of Zn and S are 51.88% and 48.12%, respectively, which gives atomic ratio of Zn:S = 1:0.92. The result of such measurement for the zinc and sulphur is shown in the inset table of figure 7. These results support that the sample ZnS has a good stoichiometric compound. Continuing with the consideration that each unit cell contains two zinc atoms and two sulphur atoms. Figure 8 proved the presence of doped material Mn.

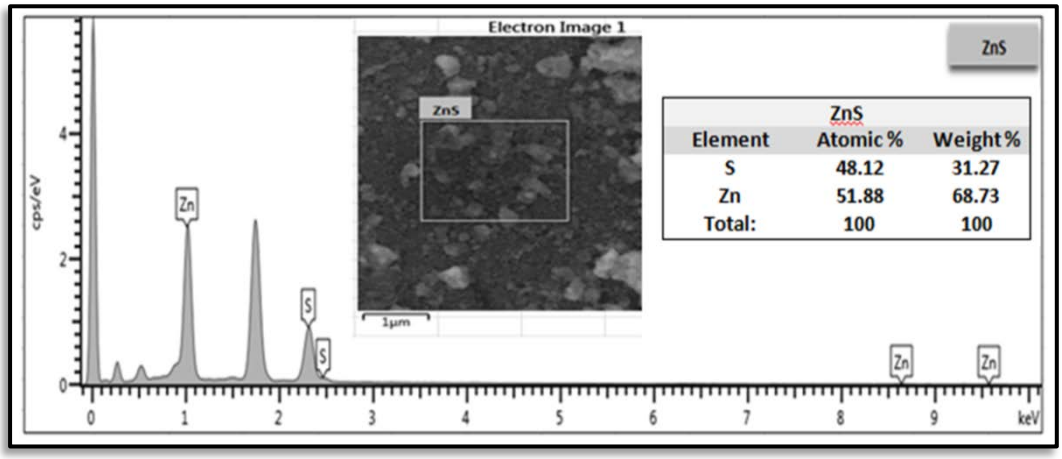

Fig.7 EDS spectrum for pure ZnS.

Fig. 8 EDS spectrum for Mn doped ZnS.

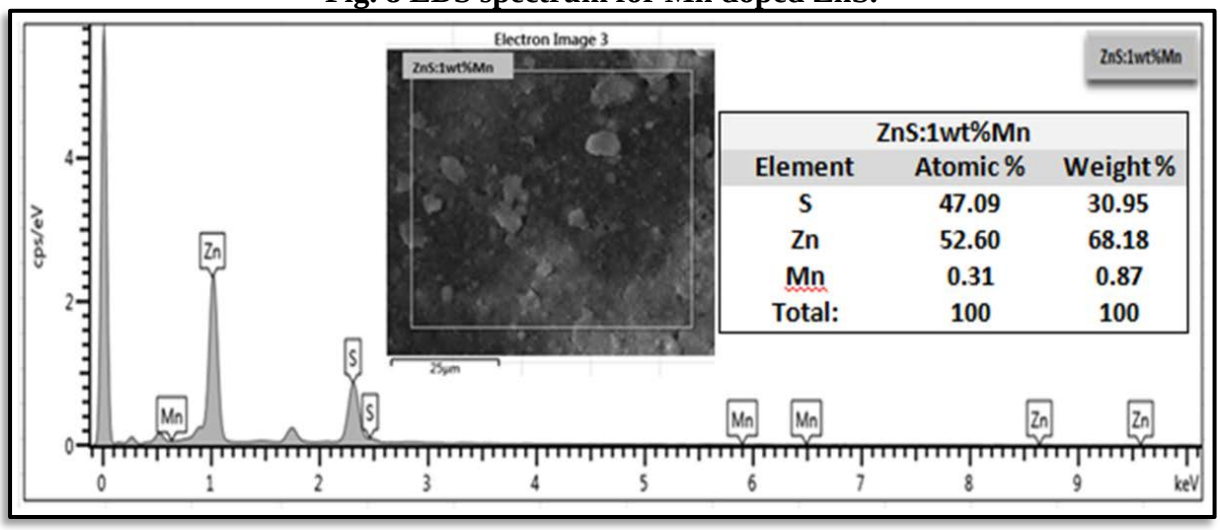

3.2 Optical properties

The optical properties of pure and doped ZnS are discussed in this paragraph. It starts with the absorption of the different samples and then shows how Tauc's relation was used to calculate the band gap of the different samples. This is followed by the photoluminescence (PL) data for the different samples.

3.2.1. Absorption

The absorption measurement was performed on the powders using UV-Vis spectrophotometer. The powders were first dispersed in distilled water and placed in a quartz cuvette. The absorption characteristics were measured after the powders were dissolved. Distilled water was used as the reference sample.

ISSN 2348 – 7968

The UV-Vis absorption spectra (Figures 9A, 10A) of the synthesized undoped and doped ZnS nanoparticles with Mn have been recorded, to measure their band-gap. ZnS has good absorption for light in the wavelength of 190-350 nm and this peak position reflects the band gap of the particles. The shoulder or peak of the spectra corresponds to the fundamental absorption edges in the samples[22], this fundamental absorption, which corresponds to electron excitation from the valence band to conduction band, can be used to determine the nature and value of the optical band gap of the prepared ZnS nanoparticles. The spectra show absorption edge of the nanoparticles in the range 241 to 329nm, showing these nanoparticles being blue-shifted as compared to bulk ZnS for which the peak is at 345 nm[23]. The blue shift in the absorption edge is due to the quantum confinement of the excitons, resulting in a more discrete energy spectrum of the individual nanoparticles. The effect of the quantum confinement on impurity depends upon the size of the host crystal. As the size of the host crystal decreases, the degree of confinement and its effect increases [24]. From figures of absorption; it can also be seen that there is no regular trend in the absorption intensity for the different wt.% samples.

3.2.2. Band gap determination

Tauc's relation (eq. 6) was applied to determine the band gap of the synthesized samples. The value of *n* is ½, because ZnS is a direct band gap material [23]. The linear part of the graph was extrapolated to $(\alpha h\nu)^{1/n} \approx 0$ to determine the bandgap.

$$\alpha h\nu = A\,(h\nu - E_g)^n \quad \text{.....(6)}$$

Where *A* is a constant which is different for different material, α is the absorption coefficient, hν is energy of incident photon, E_g is the band gap energy, and n indicates the type of transition.

From figures 9B & 10B, it was determined that the band gap of undoped and doped ZnS is greater than that of bulk ZnS (3.66 eV)[25].

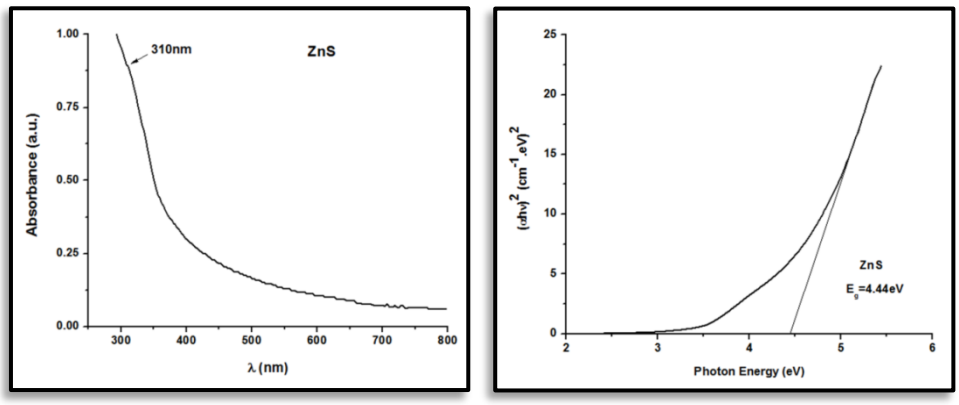

A **B**

Figure 9 A) UV-Vis absorption spectra of ZnS QDs, B) Tauc plot of ZnS QDs.

This is an indication that a strong quantum confinement happened and the particle size decreased to nm range. According to quantum confinement theory, electrons in the conduction band and holes in the valence band are spatially confined by the potential barrier of the surface. Due to confinement of both electrons and holes, the lowest energy optical transition from the valence to conduction band will increase in energy, effectively increasing the band gap (E_g) [26]. On doping Mn in the ZnS nanoparticles, it is noticed that there is red

ISSN 2348 – 7968

shift, i.e. the energy gap decreases with increasing doping concentration for Mn. Wang et al. [27] also observed similar red shift in CdS host nanocrystal with increasing Mn concentration. This might be due to the fact that Mn form new energy levels in the ZnS energy band . On increasing the doping concentration of Mn^{2+}, optical band gap reduces. This change in band gap suggests that there is direct energy transfer between the host semiconductor-excited states and the 3d levels of Mn^{2+} ions [10]. The radius of the particles can be calculated by using the mathematical model of effective mass approximation presented in eq.(7) [28]:

$$r(E) = \frac{0.32 - 2.9\sqrt{E - 3.49}}{2(3.50 - E)} \quad \text{.....(7)}$$

Where r & E are the radius and the energy gap. Using equations 6 and 7, the band-gap and average particle size of ZnS and ZnS:Mn nanoparticles have been calculated which are shown in Table2.

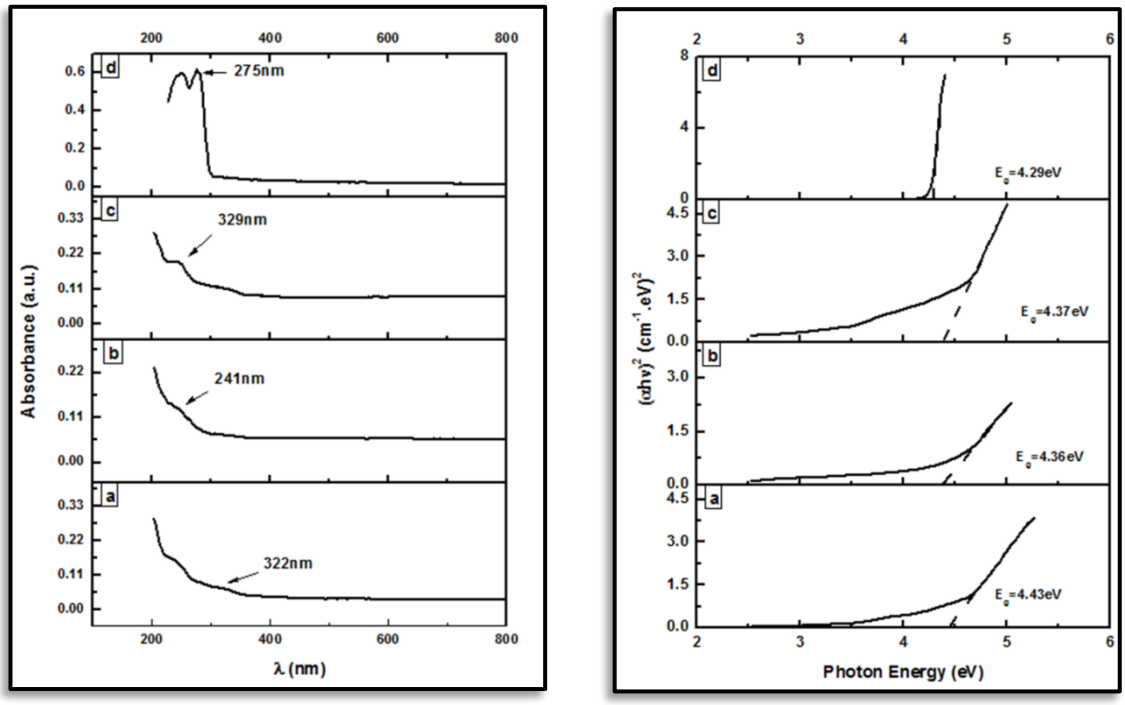

A **B**

Figure 10 (A) UV-Vis absorption spectra of Mn doped ZnS QDs, (B) Tauc plot; (a,b,c &d are corresponding to doping concentrations 1%, 2%, 3% and 4%) respectively.

Table-2 Values of Eg, absorption edge λ_e and particle radius.

Samples	Eg (eV)	λ_e (nm)	r (nm)
ZnS	4.44	310	1.33
ZnS:1wt.%Mn	4.43	322	1.33
ZnS:2wt.%Mn	4.36	241	1.38
ZnS:3wt.%Mn	4.37	229	1.37
ZnS:4wt.%Mn	4.29	275	1.43

ISSN 2348 – 7968

4. Conclusions

In summary, undoped and doped ZnS nanoparticles have been successfully synthesized via a simple microwave-assisted heating process as an easy and very fast method through the reaction between zinc acetate manganese chloride and thioacetamide as zinc, manganese and sulfur sources respectively. XRD results showed that the obtained undoped and doped ZnS nanoparticles were composed of cubic phase with very good crystallinity. The particle size obtained as smaller than 5nm using Scherer formula after extracting instrumentational and strain errors was in good agreement with HR-FESEM and optical results which is obtained by applying Brus formula.

5. References

[1] Achermann M., Petruska M. A., Kos S., Smith D. L., Koleske D. D., Ekimov V. I. Energy transfer pumping of semiconductor nanocrystals using an epitaxial quantum well. Nature 2004; 429,642-646.

[2] Huynh W. U., Dittmer J. J., Alivisatos A. P. "Hybrid Nanorod-Polymer" Solar Cells Science 2002; 295(5564) 2425-2427.

[3] S. Velumani, J.A. Ascencio, *"Formation of ZnS nanorods by simple evaporation technique"* Appl. Phys. A 79 (2004) 153.

[4] P. Yang, M.K. L¨u, D. X¨u, J. Phys. Chem. Solids 64 (2003) 155.

[5] J.F. Chen, Y.L. Li, Y.J. Yun," *Preparation and Characterization of Zinc Sulfate Nanoparticles Under High-gravity Environmental"* Mater. Res. Bull. 39 (2004) 185.

[6] Yang H, Holloway PH, Ratna BB , "*Photoluminescent and electroluminescent properties of Mn-doped ZnS nanocrystals*". J Appl Phys(2003) 93:586–592.

[7] Peng WQ, Cong GW, Qu SC, Wang ZG, "*Synthesis and photoluminescence of ZnS:Cu nanoparticles*". Opt Mater (2006)29:313–317.

[8] Sarkar, R.; Tiwary, C.S.; Kumbhakar, P.; Basu, S.; Mitra, A.K.,*"Yellow-orange light emission from Mn^{2+} doped ZnS nanoparticles*". Physica E, 40(2008)3115–3120.

[9] Fang X, Bando Y, Gautam UK, Zhai T, Zeng H, Xu X, Liao M, Golberg D, " *ZnO and ZnS nanostructures: ultraviolet-light emitters, lasers, and sensors*". Crit Rev Solid State 34(2004)190–223.

[10] Dong B, Cao L, Su G, Liu W, Qu H, Zhai H, "*Water-soluble ZnS:Mn/ZnS core/shell nanoparticles prepared by a novel tow step method*". J Alloy Compd 492(2010):363–367.

[11] Lu X, Yang J, Fu Y, Liu Q, Qi B, Lu C, Su Z, "*White light emission from Mn2 doped ZnS nanocrystals through the surface chelating of 8-hydroxyquinoline-5-sulfonic acid*". Nanotechnology21(2010)115702.

[12] Bhargava RN, Gallagher D, Hong X, Nurmikko A, "*Optical properties of manganese-doped nanocrystals of ZnS*", Phys Rev Lett (1994)72:416–419.

[13] Bhargava RN, " *Doped nanocrystalline materials—physics and applications*". J Lumin (1996) 70:85–94.

[14] B.D. Cullity, S.R. Stock, Elementary of X-ray Diffraction, Englewood Cliffs, 3rd ed., Prentice-Hall, New Jersey, 2001.

[15] John Rita and Florence S. Sasi, Structural and optical properties of ZnS nanoparticles synthesized by solid state reaction method, *Chalcogenide Letters*, 6, 535-539 (2009)

ISSN 2348 – 7968

[16] Begum Anayara, Hussain Amir and Rahman Atowar, Effect of deposition temperature on the structural and optical properties of chemically prepared nanocrystalline lead selenide thin films, *Beilstein J.Nanotechnol*., 3, 438-443 (2012)
[17] Dhanam M., Kavitha B., Jose Neetha. and Devasia Dheera. P., Analysis of ZnS nanoparticles prepared by surfactant micelle-temperature inducing reaction, *Chalcogenide Letters*, 6, 713-722 (2009)
[18] Ramasamy V., Praba K. and Murugadoss G., Study of optical and thermal properties in nical doped ZnS nanoparticles using Surfactants, *Superlattices and Microstructures* , 51, 699-714 (2012)
[19] Dhanam M., Kavitha B. and Velumani S., An investigation on Silar Cu(In1-x Alx)Se2 thin films, *Mat.Sc. and Eng. B*, 174, 209-215 (2010)
[20] Sarma K., Sarma R. and Das H.L., Structural Characterization of thermally evaporated CdSe thin films, *Chalcogenide Letters*, 5, 153-163 (2008)
[21] Tsunekawa S, Wang J T and Kawazoe Y, *J.Alloys and Compounds*, 2006, 408, 11.

[22] T. Hoa, L. Vu, T. Canh and N. Long, *J. Phys.*, 187 (2009) 012081.

[23] B.S. Rema Devi, R. Raveendran and A.V. Vaidyan, Pramana – J. Phys, 68 (2007) 685.

[24] S. Kumara, N. Verma and M. Singla ,*Chalcogenide Letters* , 8 (2011) 561.

[25] O.M. Ntwaeaborwa and P.H. Holloway, Nanotechnology 16 (2005) 867.

[26] D. Onwudiwe and P. Ajibade *Int. J. Mol. Sci.* , 12 (2011) 5538.

[27] Z. Wang, J. Zhao, L. Song, L. Shen, H. Yang, L. Wang and D. Zhang, Mater. Lett. 57, (2003) 2290.
[28] Javad Mirzaei, Mitya Reznikov and Torsten Hegmann, *"Quantum dots as liquid crystal dopants"*, J. Mater. Chem., 22 (2012) 22350-22365.